# PLIF and PIV on a 15 kHz Supersonic Co-Axial Injector

John T. Solomon<sup>1</sup>, Noah Hackworth<sup>2</sup>, Rhys Lockyer<sup>3</sup> Tuskegee University, Tuskegee, AL, 36088

With a focus on improving mixing at extreme flow velocity conditions, this paper presents planar laser-induced fluorescence (PLIF) and particle image velocimetry (PIV) studies on the flowfield of a high-speed, pulsed co-flow system integrated with a high-frequency actuator operating at 15 kHz. This active injection system delivers a supersonic pulsed actuation air jet at the inner core of the co-axial nozzle that provides large mean and fluctuating velocity profiles in the shear layers of a fluid stream injected surrounding the core through an annular nozzle. The instantaneous velocity, vorticity, and acetone concentration fields of the injector in three distinct modes of operation – pulsed actuation, steady actuation, and without actuation -are presented. The high-frequency streamwise vortices and shockwaves tailored to the mean flow significantly enhanced supersonic flow mixing between the fluids compared to the steady co-axial configuration operating at the same input pressure. The study analyzes the mixing and dynamic characteristics of this active co-axial injection system, which has the potential for supersonic mixing applications.

#### I. Introduction

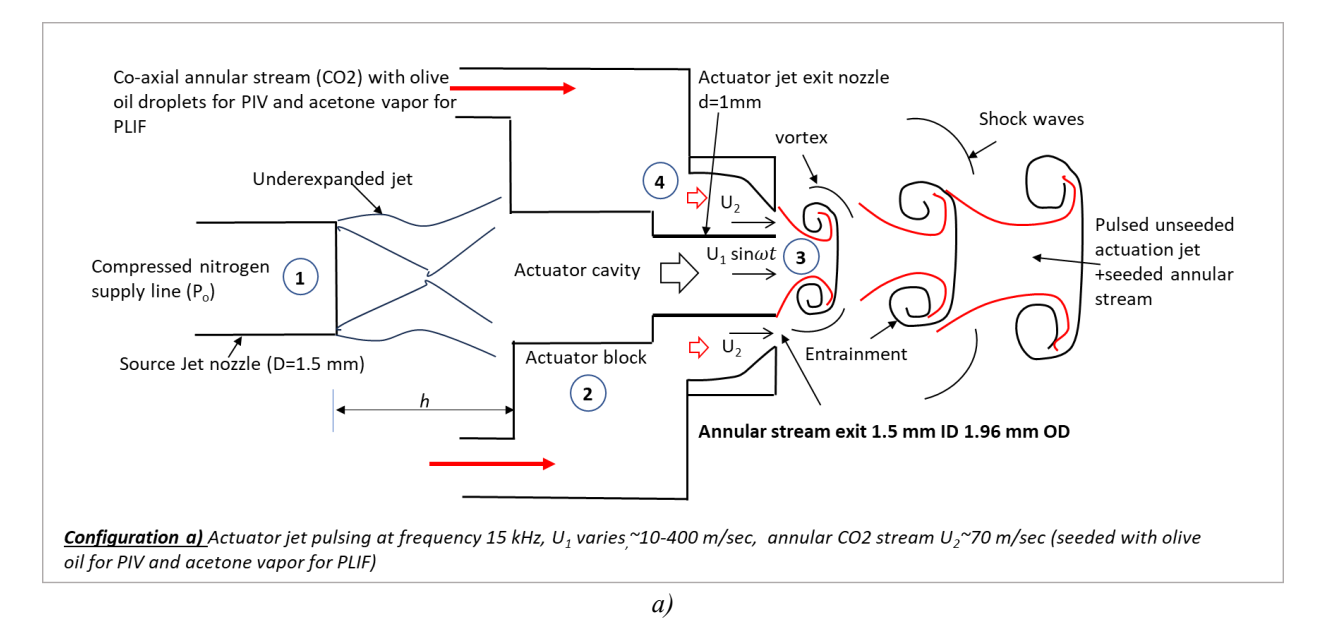
A co-axial jet configuration is a simple and effective mixing enhancement method in which fluids flowing separately through the inner core and the annular space meet at the exit plane of the injector nozzle assembly. For example, in applications like a gas turbine or combustion chamber of a rocket engine, these fluids could be oxidizers, such as gaseous or liquid oxygen, and fuel in its liquid or gaseous phase. Effective and controlled mixing can lead to higher combustion efficacy, longer life, reduced combustor size, stable operations, and fewer emissions/pollutants. Although the mixing ultimately happens at the molecular level, active flow control techniques can tailor the flow dynamics at micro and macro scales of such systems in favor of rapid diffusion at the molecular level [1-3]. A major challenge for mixing in such extreme flow conditions is the microscopic convective time scale (order of milliseconds) associated. Such a smaller time scale demands robust flow control actuators that enhance microscale mixing at high speed and positively alter the macroscopic phenomena associated. The entrainment and vorticity dynamics resulting from the shear layer instability modification play a significant role in the overall efficiency of the mixing process. Passive methods proposed for improved mixing in high-speed systems use flush-mounted or intrusive injectors to generate streamwise, counter-rotating vortices for rapid nearfield mixing of the incoming air and fuel [4-12]. Beyond the classical passive co-axial configuration, a few studies explore active schemes such as powered resonance tubes (PRT) or Hartmann-Sprenger tubes as an option to excite the shear layer at high frequency [13].

Fig. 1 shows a schematic of the active co-axial injector used in this study, indicating its essential components and three modes of operation. The injector assembly shown in Fig. 1a has four major elements: 1) compressed air from a source nozzle enters, 2) an actuator block, 3) a pulsed supersonic jet flows out of the actuator block, and 4) the fluid stream that flows out co-axially surrounding the actuation jet. 1. Both the fluids meet co-axially at the exit plane of the assembly, as shown in fig 1a.

1

<sup>&</sup>lt;sup>1</sup>Professor, Department of Mechanical Engineering, Senior Member AIAA

<sup>&</sup>lt;sup>2,3</sup> Research Assistant



Co-axial steady stream seeded with olive oil droplets for PIV and acetone vapor for PLIF

Configuration b) Steady actuation jet without pulsing U<sub>1</sub>~ 400 m/sec & seeded annular stream U<sub>2</sub>~ 70 m/sec

Co-axial steady stream seeded with olive oil droplets for PIV and acetone vapor for PLIF

Co-axial steady stream seeded with olive oil droplets for PIV and acetone vapor for PLIF

Co-axial steady stream seeded with olive oil droplets for PIV and acetone vapor for PLIF

Co-axial steady stream seeded with olive oil droplets for PIV and acetone vapor for PLIF

Co-axial steady stream seeded with olive oil droplets for PIV and acetone vapor for PLIF

Co-axial steady stream seeded with olive oil droplets for PIV and acetone vapor for PLIF

Co-axial steady stream seeded with olive oil droplets for PIV and acetone vapor for PLIF

Co-axial steady stream seeded with olive oil droplets for PIV and acetone vapor for PLIF

Co-axial steady stream seeded with olive oil droplets for PIV and acetone vapor for PLIF

Co-axial steady stream seeded with olive oil droplets for PIV and acetone vapor for PLIF

Co-axial steady stream seeded with olive oil droplets for PIV and acetone vapor for PLIF

Co-axial steady stream seeded with olive oil droplets for PIV and acetone vapor for PLIF

Co-axial steady stream seeded with olive oil droplets for PIV and acetone vapor for PLIF

Co-axial steady stream seeded with olive oil droplets for PIV and acetone vapor for PLIF

Co-axial steady stream seeded with olive oil droplets for PIV and acetone vapor for PLIF

Co-axial steady stream seeded with olive oil droplets for PIV and acetone vapor for PLIF

Co-axial steady stream seeded with olive oil droplets for PIV and acetone vapor for PLIF

Co-axial steady stream seeded with olive oil droplets for PIV and acetone vapor for PLIF

Co-axial steady stream seeded with olive oil droplets for PIV and acetone vapor for PLIF

Co-axial steady stream seeded with olive oil droplets for PIV and acetone vapor for PLIF

Co-axial steady stream seeded with olive oil d

Fig. 1 Schematic of the pulsed co-axial injector system and its operating modes a) Pulsed co-axial flow b) steady co-axial flow c) Annular flow alone without actuation

In the pulsed mode of operation, the inner actuation jet velocity U1 varies periodically from ~0-400 m/sec at a design frequency of 15.5 kHz, providing a highly unsteady velocity profile to the annular flow at the exit, as indicated in Fig. 1a. To achieve pulsed mode, the parameter h/D is kept at 1.3 where h is the distance of source nozzle from the actuator, and D is the diameter of source jet. The source pressure is maintained at 65 psi, with a nozzle pressure ratio NPR = 5.8. In this mode, the instabilities of the injected co-flowing fluid can be tailored using the pulsed supersonic actuation jet operating in a frequency range of 1-60 kHz [19]. The co-axial annular stream exits with a constant velocity of U2, depending on the injection pressure. The annular stream velocity is kept at 70 m/sec for the present experiments. In the pulsed actuation mode of operation, the shear layer of the annular fluid is exposed to the ambient air on one side and the central pulsing jet on the other. Fig. 1b shows a representative flow pattern of the flowfield at the exit when the nozzle assembly operates in a steady actuation mode. This mode of operation can be achieved by placing the source jet (element 1 in Fig. 1a) flush with the actuator cavity where h/D = 0. In this case, the steady annular coaxial jet interacts with an under-expanded central actuation jet at the nozzle exit. Fig. 1c shows flow features when the injector operates in *no actuation* mode. Only the annular stream flows through the injector in this mode of operation. The source jet pressure is maintained at 0 psi in this case. More details of the actuator used in the co-axial configurations, its early development, and prior implementation for various high-speed flow control applications are available in [14-21].

A recent study by Solomon et al. (AIAA J 2023) on this configuration using PLIF indicates that mixing has significantly increased between the annular fluid and the actuation jet when the nozzle system operates in a high-frequency pulsing actuation mode compared to a classical steady, co-axial actuation mode [22]. The present paper further analyzes this interesting observation using the instantaneous velocity, vorticity, and concentration field measurement of the injector assembly in three operation modes indicated in Fig. 1. The goal is to analyze the flow dynamics using PIV and to understand its connection to the enhanced flow mixing characteristics captured using PLIF.

### II. Experimental Details

### A. Facility Description

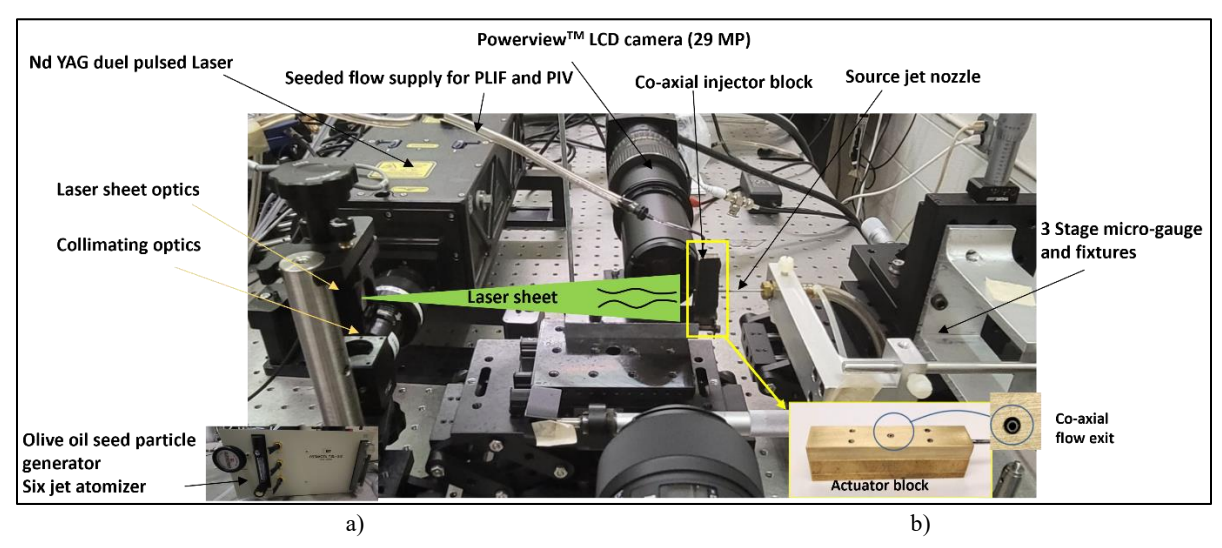


Fig. 2 PLIF and PIV setup established at Tuskegee University for the present study

## a) Set up for particle image velocimetry (PIV) and planar laser-induced fluorescence (PLIF)

The PIV and PLIF imaging uses a setup, as shown in Fig. 2, established recently at Tuskegee University with support from the US National Science Foundation. The critical component of this setup is a Quantel EverGreen<sup>TM</sup> Nd-YAG dual pulsed laser with a choice of pulse energies up to 200 mJ at 532 nm and 30 mJ at 266 nm with a repetition rate of 15 Hz. PIV experiments use laser pulses at 532 nm. PLIF experiments use laser pulses at 266 nm. A Powerview<sup>TM</sup> LS-LCD camera (29 MP, 6600x4400) with high quantum efficiency, low noise with 1.8 frames/s, selectable 12-bit or 14-bit output, and 100 mm f/2.8 camera lens with appropriate filters, acquires the images. An eight-channel digital laser pulse synchronizer with 250 ps resolution controls the laser pulses and the trigger for the camera. A UV optic periscope and adjustable laser sheet optics (LSO) with 266/532 mm AR coat create a thin laser sheet at an appropriate test plane in the flowfield generated by the pulsed co-axial assembly. A six-jet atomizer-9306 TSI<sup>TM</sup> generates olive oil droplet seeding in the annular CO2 stream for PIV measurements. For PLIF measurements, another six-jet oil droplet generator-9307-6 TSI<sup>TM</sup> was used for generating acetone vapor seeding the annular stream of CO2 gas.

#### b) PIV Data acquisition and processing method

The PIV image acquisition and analysis used INSIGHT4G<sup>TM</sup> software. Figure 3a shows representative instantaneous raw images of the flowfield with olive oil seed particles at three different modes of operation as described earlier in Fig. 1. Fig. 3a (i) is an instantaneous phase of the annular seeded jet actuated with a high-frequency actuation jet operating at 15.5 kHz when the source jet nozzle maintained at 65 psi. The inner diameter (ID) of the annular nozzle is 1.96 mm. The actuation jet exits from a nozzle of 1mm ID and 1.5 mm OD, which gives an annular exit dimension of 1.5 mm diameter and 460-micrometer thickness, as indicated in Fig. 3. Adjusting the parameter h/D, the actuation mode can be switched from steady to pulsing at the same input pressure. At this pressure, the actuation jet velocity at the exit is sonic (~350 m/sec). As an under-expanded jet, the actuation jet expands to supersonic speed (~400 m/sec) outside the co-axial assembly. Fig. 3a (iii) shows the annular seeded jet actuated with a steady actuation jet from a source nozzle maintained at 65 psi. Fig. 3a (iii) corresponds to a seeded annular jet at an exit velocity of 70 m/sec without a co-flowing actuation jet at the center.

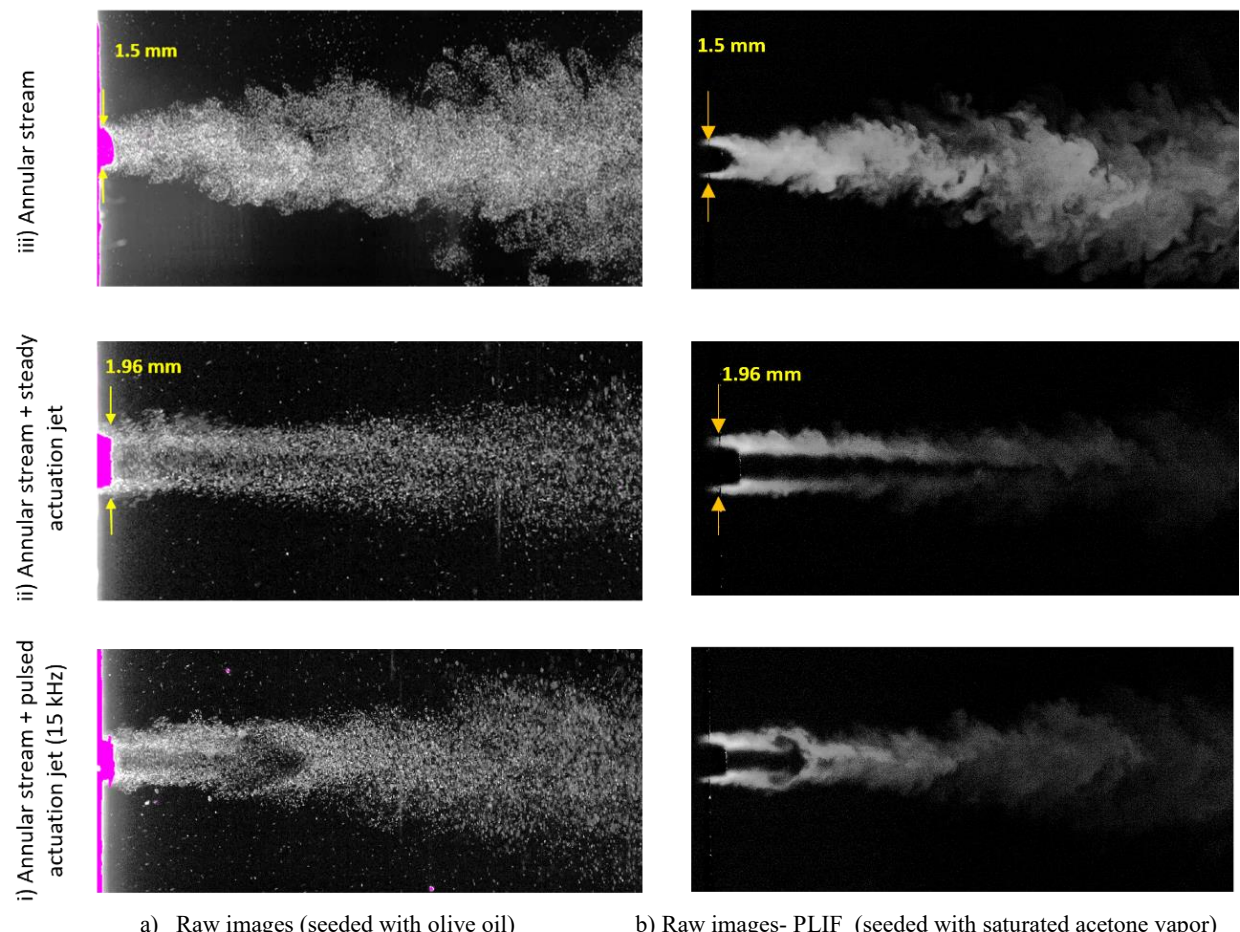


Fig. 3 Representative instantaneous raw images of the flowfield at three different modes of operation

The field of view for PIV measurement is 20 mm across the flow and 50 mm in the streamwise direction. The major challenge for image acquisition is the flow scale (order of mm) and the higher speed of the co-axial stream resulting from the supersonic jet actuation. The actuation jet in steady mode operates at a supersonic speed of 400+ m/sec. The pulsing actuation provides a velocity fluctuation of ~10-400 m/sec to the particle-seeded annular flow. The image acquisition parameters, such as time between the laser pulse (Δt), laser pulse delay, and PIV exposure time, were fine-tuned considerably to achieve image pairs with sufficient particle movements in various operating conditions. For the steady and unsteady actuation cases, the Δt is chosen at 0.40 microseconds, which will give 157 micrometers  $(\mu m)$  movement of seed particles at a velocity of 350 m/sec. Since the image resolution of the camera is 23  $\mu$ m/pixel, the seed particle will move at least 6-8 pixels distance at this measurement speed. The  $\Delta t$  is chosen at a higher value of 2 µs for measuring the low-velocity field of the annular flow moving at 70 m/sec near the injector exit. The laser pulse repetition rate was kept at 1.5 for all measurements. Since the Δt of the laser is extremely short at 400 nanoseconds, and the camera shutters have to close and adjust with the signals physically, there exists an actual delay in the timing for the camera exposure as opposed to the observation in the timing diagram. The laser pulse delay time is fine-tuned to keep the two camera exposures in sync with the double laser pulses with the extremely short  $\Delta t$ . For 2D spatial calibration, a measured distance in the image -the outer tube diameter is 1.5 mm, measured within the image and used for calibration. A background removal technique generates cleaner and continuous vector fields during preprocessing. This technique uses the *Image Generator* plugin to calculate the minimum pixel intensity of the input images. This minimum intensity is subtracted from the raw images by the *Image Calculator*, which sets its operation parameter to subtraction and its operand parameter to the image and passes in the generator image. An appropriate processing mask is used for processing data in a region of interest 19 pixels from the nozzle. More details of the PIV image processing method are available in reference [21]

#### c) PLIF data acquisition and processing

For PLIF data acquisition, the annular stream is seeded with saturated acetone vapor from the six-jet oil droplet generator-9307-6TSI<sup>TM.</sup> The PLIF measurement uses an ultra-thin laser sheet of 266 nm wavelength to fluoresce the absorbing species (acetone) in a given measurement volume. Many studies report that acetone fluorescence has a linear variation with concentration and laser power [23, 24]. Acetone absorbs ultraviolet light (225 - 320 nm) but fluoresces in the blue (350 - 550 nm). This study uses CO2 as an annular stream and compressed nitrogen for generating high-frequency actuator jet pulses. Since the resulting fluorescence is proportional to the amount of the absorbing species in the measurement volume, measuring the intensity of light from the fluorescent molecules captured using an appropriate camera with a filter will quantify the mixing of the annular stream with the unseeded actuation jet. The mixture fraction calculated at each location usually represents the mixing characteristics of the flow. From raw images, the intensity of acetone in the flowfield is analyzed using MATLAB<sup>TM</sup> and INSIGHT4G<sup>TM</sup> software.

#### d)Measurement uncertainties

The source jet pressure measurement has an uncertainty of 0.1 psi. The micro-gauge used for linear movements of the nozzle block for varying the parameter h/D has an uncertainty of 0.01 mm. A TSI<sup>TM</sup> Mass Flow Multi-Meter 5300-4 measures the flow rate CO2 with 2% reading accuracy for measurements up to 300L/min. A high-pressure compressed nitrogen tank (2000 psi) supplies air to the source jet nozzle and the pulsed jet injector assembly. A multi-channel oscilloscope monitors all signals used for measurements for accuracy. The uncertainty of velocity measurements in PIV is estimated from 3-13% (using the INSIGHT4G<sup>TM</sup> software) when the particle speed ranges from low subsonic (20 m/sec) to supersonic (400 m/sec).

# B. Design details of the co-axial injector assembly

Figure 4 shows the design details of the pulsed co-axial injector assembly (actuator block indicated in Figure 1) fabricated with three brass plates. The top plate contains a 3mm long, 1.3 mm diameter cavity through which an underexpanded actuator source jet enters the nozzle block. The second plate has another internal hole that forms the boundary for the resonance phenomena. 1 mm (ID) steel tube (with 1.5 mm OD) connects the cavity in the second plate and directs the air jet to flow out from the base of the third plate. The last plate has a 1.96 mm orifice, so when combined with the second plate and the steel tube with 1.5 mm OD, an annular space is formed outside the 1mm tube (ID). The internal cavity in plate 3 connects to a steady fluid (CO2) supply line through a steel tube. The design ensures no interaction or coupling between the co-axial fluids before they reach the exit plane of the assembly.

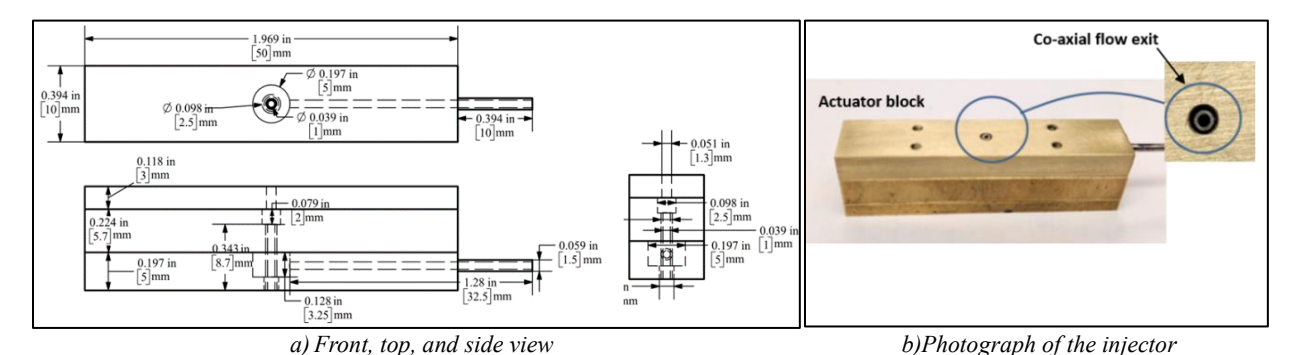


Fig. 4 Design details of the co-axial injector a) front, side, and top views b) Photograph of the pulsed co-axial injector

This assembly has a total internal cavity volume of 20.6 mm<sup>3</sup>. An under-expanded source jet supplied from a nozzle of 1.5 mm exit diameter (D) enters the assembly through a 1.3 mm orifice located on the first plate. This source jet produces pulsed flow through the 1mm diameter tube integrated into the second and third plates under suitable resonance conditions. This design allows olive oil-seeded or acetone-seeded fluid stream (CO2) injection through the annular space while the central tube delivers a pulsed or steady actuation air jet (N2). Experiments use two control parameters, h/D or nozzle pressure ratio, NPR, for frequency control. The present study uses h/D =1.3 and NPR =5.8 to achieve a pulsing frequency of 15.5 kHz.

### **II Results and Discussions**

#### A) Frequency characterization of the pulsed co-axial assembly

Figure 5 shows the frequency spectra of the actuator integrated into the nozzle assembly measured using a

GRAS<sup>TM</sup> 1/4-inch Free-Field Microphone with a sensitivity of 4 *mV/Pa*. National Instruments<sup>TM</sup> 9234, 24-bit, 51.2 kHz data-acquisition module acquires the microphone data using LabVIEW<sup>TM</sup>.

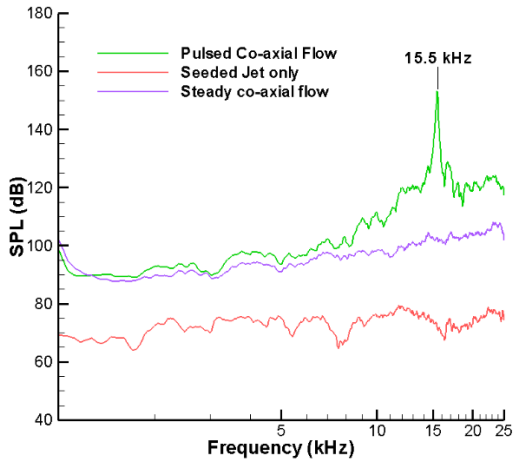


Fig. 5 Spectra of the actuator at three modes operation-pulsed, steady, and no actuation

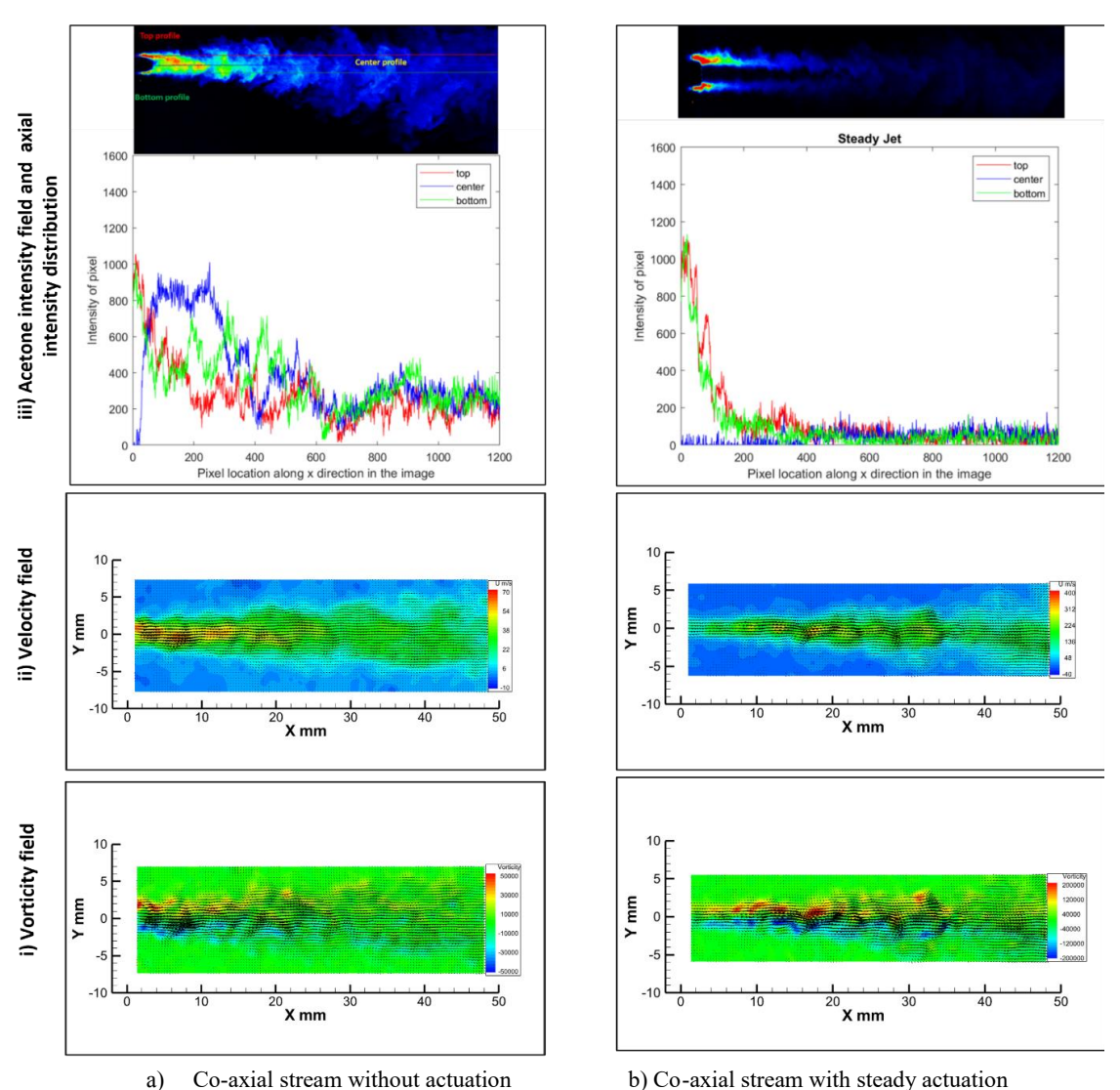
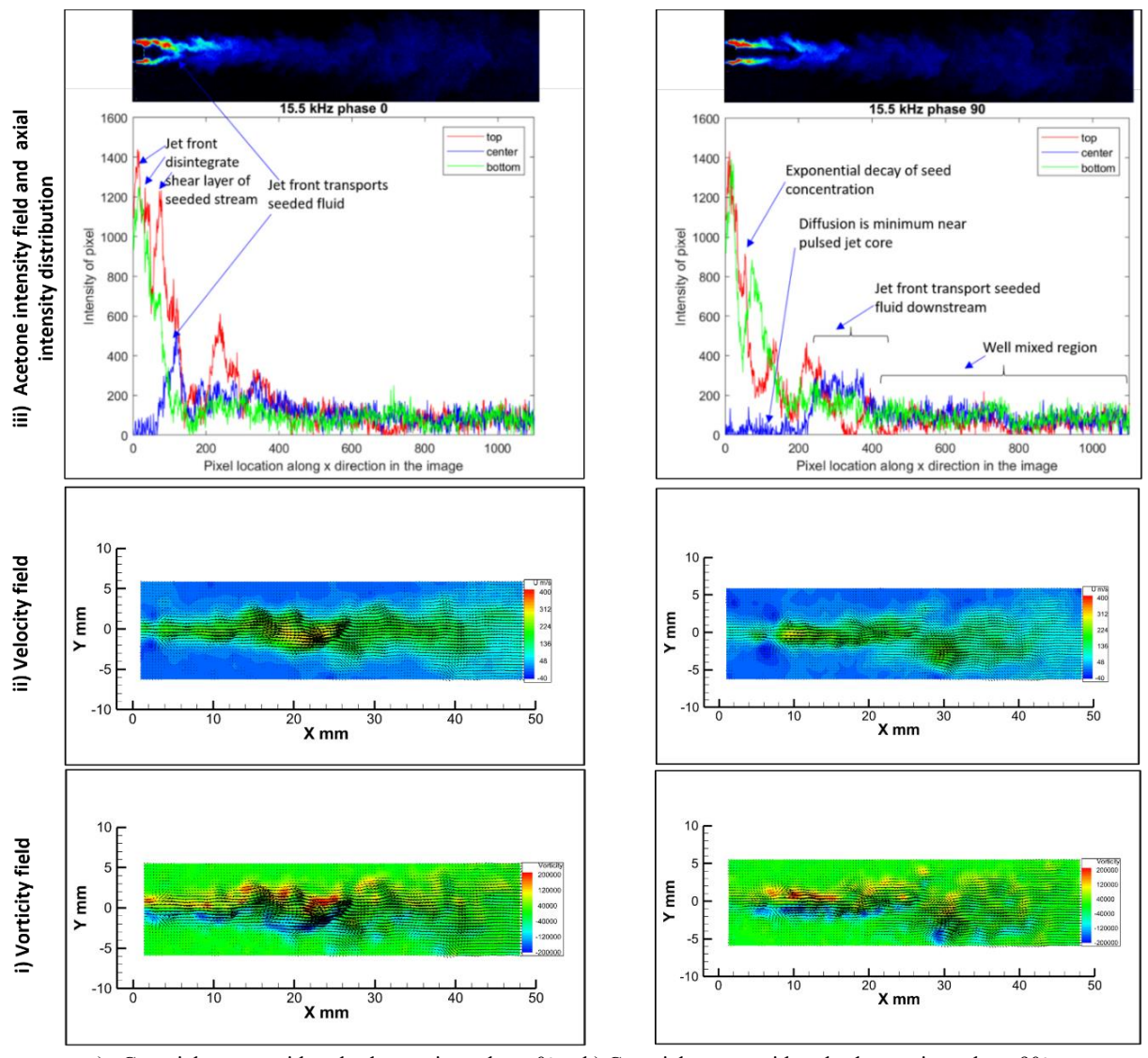


Fig. 6 Instantaneous velocity, vorticity, and acetone concentration fields of the seeded annular stream

Fast Fourier transformation (FFT) of time series with 2048 data points and Hanning window with 50% overlap compute acoustic spectra used in the analysis. The pulsed co-axial flow shows a distinct frequency at 15.5 kHz, while the steady co-axial injection shows no specific tones in the spectra other than broadband noise. In steady actuation, energy is in broadband and is focused at 15.5 kHz for pulsed actuation. The spectra of the seed jet show low amplitude broadband noise, indicating natural instabilities in the flow. The present experiments use pressure and the flow rate of CO2 (annular stream) at 8 psi and 4.7 lit/min, respectively. For a given annular exit area of 1.08 mm², this flow rate gives an estimated exit velocity of U2  $\sim$ 70 m/sec for the seeded CO2 jet. The exit velocity U1 of the pulsed jet varies 10-400m/sec during the cycle, giving rise to a range for velocity ratio U1/U2 $\sim$ 0-6. The exit flow area ratio A1/A2 of the present configuration is 0.72, where A1 is the area exit of actuator flow, and A2 is the area of the annular space. With a pressure ratio of fluids exiting the assembly ( $P_{act}/P_{stream}$ ) that varies in the range of 1-13 during the pulsed co-axial injection process, the momentum of the actuation jet dominates the flowfield for most of the pulsing cycle.



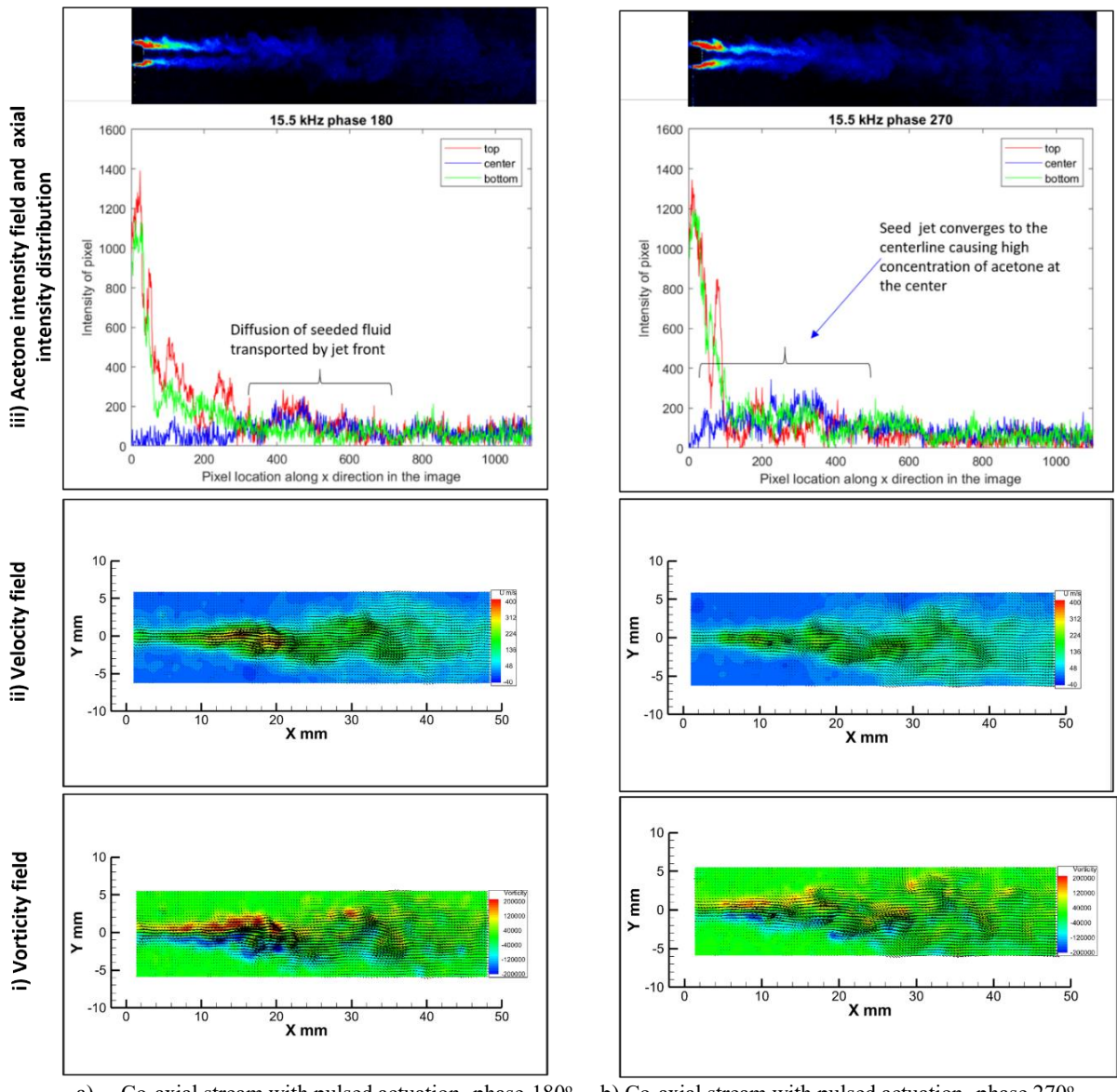
a) Co-axial stream with pulsed actuation- phase-0° b) Co-axial stream with pulsed actuation- phase 90° Fig. 7 Instantaneous velocity, vorticity, and acetone concentration fields of the seeded annular stream

#### B) Instantaneous PLIF and PIV field (acetone concentration, velocity, and vorticity)

a) Subsonic seeded annular flow without co-axial actuation jet

Figure 6 *a (iii)* shows a representative instantaneous PLIF image of the annular stream where acetone acetone-seeded CO2 stream is injected through the co-axial assembly without an actuation jet, and the streamwise intensity profiles of this image at three selected locations as marked in the figure. Ideally, the saturated vapor exiting the nozzle fluoresces with maximum intensity (red color in PLIF image) and unseeded actuation jet and ambient air with zero

intensity (black color in PLIF image). The maximum intensity is observed at the exit plane with a value of ~1000, and the minimum value of 0 is noted at a location just outside the nozzle before the annular stream converges at the center. Note that this is a small pocket of air without acetone seed. Assuming a linear variation between these two extreme values, the intensity of light fluorescence measured at a given location represents the local mixing of acetone with the surrounding unseeded streams. The high magnification optics and a high-resolution camera (27 MP) capture fine details of these high-speed microscale flows and their mixing characteristics in the PLIF images. For seed jet at 4.7 psi and 5 lit/min, images show the formation of a saturated core up to 20 diameters. The intensity of annular flow at the center line of the stream is measured as ~800 for the core, then drops to 200 far downstream. The jet stream then seems to mix well with the ambient air further downstream by the natural diffusion mechanism. The PLIF profile at the center (blue curve) shows the distribution of seed particles in the streamwise direction. The red and green profiles show the streamwise distribution of seed particles at the top and bottom center locations of the co-axial stream, as indicated in Fig. 6a (iii). These PLIF profiles represent the acetone concentration in the flow at various locations and provide information on its distribution in the flowfield. All the profile curves show the same intensity value of ~200, indicating well mixing with the unseeded ambient air far downstream locations. The discrete peaks and varied intensity profiles at the top and bottom locations indicate unsteadiness and instabilities in the shear layer of the annular stream.



a) Co-axial stream with pulsed actuation- phase 180° b) Co-axial stream with pulsed actuation- phase 270° Fig. 8 Instantaneous velocity, vorticity, and acetone concentration fields of the seeded annular stream

Figure 6a (ii) shows a representative instantaneous velocity field of the seeded annular flow without a co-axial actuation jet. The annular stream from the nozzle merges to form a continuous jet with a maximum stream velocity measured up to 70 m/s. The merged jet core of the annular stream is visible up to 20 mm from the exit. The stream slowly dissipates into the ambient air, and the velocity drops to 10-20 m/sec at 30 mm from the injector exit. The instantaneous velocity field also captures the natural instabilities present in the shear layer of the annular flow. Fig. 6a (i) indicates the vorticity field of the injector corresponding to velocity vectors shown in Figure 6a (ii). The top and bottom annular flow regions form a vorticity core with a maximum magnitude of ±50000/s. Beyond this length, the vorticity core disintegrates and dissipates to a lower magnitude. Note that the annular stream experiences shear on both the inner and outer sides of the stream.

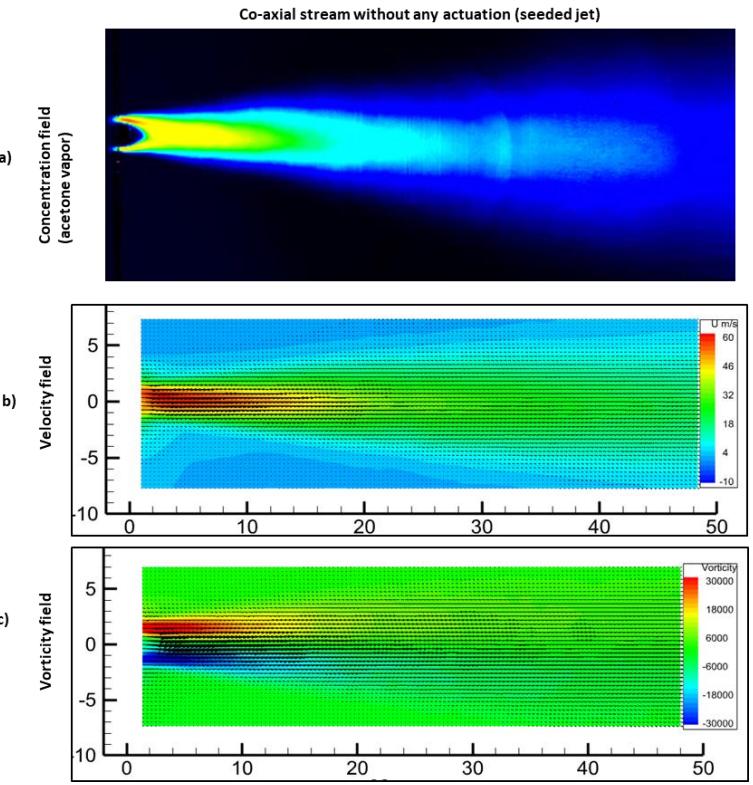


Fig. 9 Average velocity, vorticity, and acetone concentration fields of the annular stream without actuation

## b) Subsonic seeded annular flow with steady co-axial actuation jet

Fig. 6b (*i-iii*) shows representative instantaneous acetone intensity, velocity, and vorticity fields of the seeded annular flow with steady jet actuation at the center. An underexpanded jet at NPR=5.8 is used for steady supersonic actuation. The steady jet actuation accelerates and entrains the acetone-seeded annular flow as it moves downstream. Fig. 6b(iii) shows minimal entrainment near the nozzle exit. The highly underexpanded characteristic of the actuation jet and the strong compressible shear layer restrict diffusion of the seeded annular stream near the nozzle exit. The intensity of acetone is observed with a value of 1000 at the top and bottom profiles, similar to that of the annular stream without actuation discussed in Fig. 6a (iii). Due to steady jet actuation, the seed particles in the annular stream attain a maximum speed of 400 m/sec at the core after moving through a distance of 5 to 20 mm from the nozzle exit, as observed in the velocity field shown in Fig. 6b(ii). The overall velocity of the annular stream is increased significantly due to the high-momentum steady actuation jet.

Figure 6b (i)shows the corresponding instantaneous vorticity field of the seeded annular jet actuated with the steady under-expanded jet. As expected, the actuation causes continuous and intensive double vorticity streaks in the annular stream in the streamwise direction. The high vorticity magnitude (200,000/s) indicates that the actuation jet imparts intensive shear to the annular stream at the core. The magnitude of maximum vorticity has increased 4 times due to the steady jet actuation at the center core of the annular stream. The continuous vorticity streaks have extended up to 20 mm in the streamwise direction. The data quantitatively confirms the effects of steady actuation that significantly increased the velocity and vorticity of the annular fluid in the streamwise direction. The impact of this

flow dynamics modification is visible in the intensity profile shown in Fig. 6b (iii). The steady actuation resulted in a sudden drop in the acetone intensity of the annular flow from value 1000 to 100 from the exit to 10d downstream location compared to the case without actuation, where the drop is seen more gradually and over a distance of 20d from the exit. The intensity value at the center of the actuation jet is almost zero until 20d from the exit due to its coherent structure with shock patterns that prevent diffusion of the acetone-seeded annular stream into its core. The slowdown of the actuation jet further downstream allows some mixing with the annular acetone-seeded jet. A high-velocity actuation jet quickly reduces the intensity of annular flow, as observed in Fig. 6b (iii).

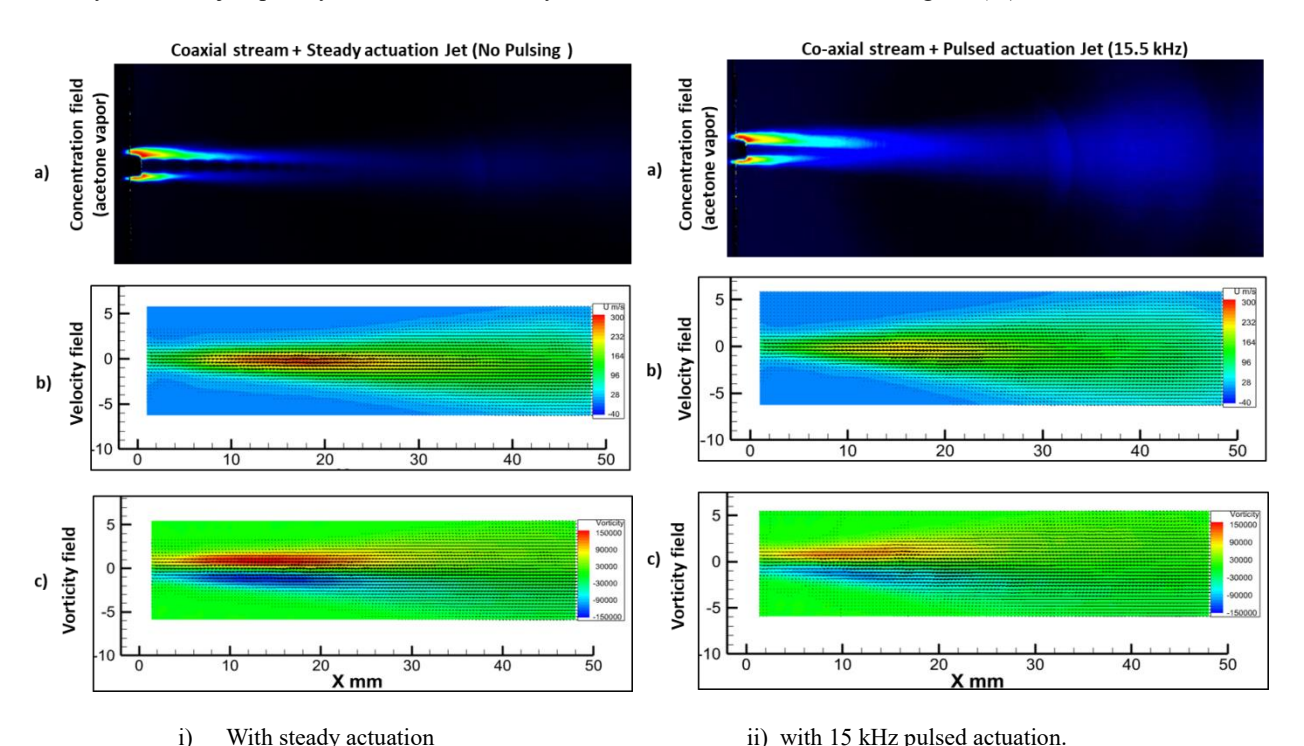


Fig. 10 Average velocity, vorticity, and acetone concentration fields of the annular stream

c) Subsonic seeded annular flow with supersonic pulsed co-axial actuation at 15.5 kHz

Figures 7a&b & 8a&b show instantaneous acetone intensity, velocity, and vorticity fields for four different pulsing phases of a co-axial seeded annular stream when the actuation jet pulses at 15.5 kHz. Figure 7a represents the instantaneous fields at the beginning phase (0°) of the pulsed actuation observed with an evolving vortex near the nozzle. This vortex evolves, grows, and moves downstream in the streamwise direction in phase 90°, as observed in Fig. 7b. As evident in phase 180°, as shown in Fig. 8a, the growth and entrainment of annular fluid increase as it moves further downstream. At phase 270° (Fig. 8b) pulsed vortex weakens considerably with interaction with the annular fluid and the air in the ambiance. The representative PLIF and PIV fields of pulsed actuation at various phases of actuator operation confirm that the active injection offers significant velocity fluctuations in the mean flow of annular fluid. For example, in comparison of instantaneous images at phases 90° and 180° reveals velocity fluctuations in a range of ~100-400 m/sec in the streamwise location 10-20 mm from the nozzle exit. The evolving vortex, its growth, and its movement downstream in the streamwise direction are captured in all these images. Such a highly unsteady vorticity field leads to enhanced mixing between the annular fluid and the high-velocity actuation jet. The maximum magnitude of the vorticity is observed to be the same in both steady and pulsed actuation cases.

The intensity profiles at the center (blue curves) of four different phases of pulsed actuation (0°, 90°, 180°, and 270°) in Figures 7a(iii), 7b(iii), 8a(iii), and 8b(iii) shows an interesting phenomenon of annular fluid transport by the evolving vortex of the actuation jet. The shear layer intensity profiles (red and green curves) with discrete peaks indicate that a disintegrated the shear layer of the acetone-seeded annular stream. The shock wave that precedes the evolving vortex of the actuation stream might be responsible for this breakdown. The vortex front entrains and transports the acetone-seeded annular stream, as indicated in Fig. 7a(iii). The instantaneous phase at 90° (Fig. 7b(iii) shows the further movement of this entrained transportation of the annular stream to 10d-20d downstream. The

diffusion and growth of the vortex cause a drop in intensity value from 400 to 200. At 180°, the vortex diffuses further, resulting in a lower intensity, as seen in Fig. 8a(iii). Figure 8b (iii) shows the final phase 270°, where the actuation jet velocity drops and the annular stream momentum predominates the flow domain with a relatively diffused acetone intensity and increased mixing characteristics at the center.

#### a) Averaged PLIF and PIV flowfield images and mixing characteristics

Figure 9a-c shows the averaged acetone intensity, velocity, and vorticity fields of 260 images of annular fluid without actuation. Fig. 10 i&ii presents the same for annular fluid without and with pulsed actuation. Due to the steady actuation, the core of annular fluid velocity and vorticity fields extended significantly from the nozzle exit in the streamwise direction. The maximum value of vorticity magnitude increases to 400% due to steady jet actuation and the velocity from 70 to 300 m/sec. A comparison of Fig 10i and 10ii shows pulsed actuation leads to lower average velocity for annular stream than steady actuation. This observation is as expected due to the vortex formation in the pulsed flow. The average intensity of the vorticity field was also reduced in this case, as evident from Fig. 10i(c) and 10ii(c). The steady and pulsed actuation cases show two distinct patterns of annular stream diffusion. The high momentum steady actuation jet entrains the annular fluid to its core and increases speed to supersonic with less diffusion to ambient air. Its diffusion characteristics increase as the velocity decreases beyond 30 mm from the exit. For pulsed actuation, entrainment and diffusion begin at the nozzle exit and progress uniformly in the streamwise direction due to the evolving compressible vortex. This process leads to a more diverging flowfield and attributes enhanced mixing characteristics than steady actuation.

Since each instantaneous image contains information on 4-5 cycles, the average image represents information on ~1000 cycles for the pulsed injection case. These averaged images provide a comprehensive view of all three cases' mixing characteristics and provide reasonably accurate quantitative estimates of mixing effectiveness between the cases. The intensity of each pixel in the averaged PLIF image is proportional to the average acetone concentration around that elemental volume for the image sequences selected. An average of all pixel intensity estimates acetone concentration in a given field of view for a particular case. For the first case, seed jet alone, this number is 44.3. For the second case, when an unseeded steady actuation jet flows through the core, the acetone content we measure as average intensity in the same field of view changes due to fast relative motion between the streams. The average intensity of pixels measured for this case is 7.5. The same calculation for pulsed injections shows this average intensity value as 15.9. This calculation estimates that the mixing effectiveness of pulsed co-axial injection is 114% more than the steady co-axial injection. The enhanced mixing characteristics of the pulsed co-axial injection system are attributed to the entrainment and growth of high-frequency vortex generated by the pulsed jets and through the shock wave diffusion through the interface of the seeded and unseeded flow downstream.

#### **IV Summary**

The paper presents a PLIF and PIV study on an active, supersonic co-axial jet injection assembly integrated with ultra-high frequency pulsed microactuators. The assembly steadily injects a fluid through a 460µm annular space around a 1 mm ID, 1.5 mm OD sonic nozzle with an exit velocity of 70 m/sec. The co-axial nozzle at the center (1 mm ID) issues the supersonic actuation jet in two operation modes: a) as steady under expanded jet at 65 psi and b) as pulsed actuation jet operating at 15.5 kHz at the same input pressure. The annular stream seeded with saturated acetone vapor is used for PLIF imaging and mixing studies. The velocity and vorticity field of annular fluid seeded with olive oil with and without actuation were measured using particle image velocimetry (PIV). The steady actuation has increased the velocity up to 400 m/sec and introduced four times intensive shear and extended vorticity streaks in the annular stream. The pulsed actuation resulted in fast-moving, high-frequency compressible air vortices in the injected flowfield. The growth and entrainment of these pulsed vortexes cause a highly unsteady velocity field and vorticity streaks in the annular stream. The current study confirms that the co-axial injector operating in supersonic pulsed mode can provide tailored vorticity in fast-moving fluids and enhance mixing more than 100% than a stream actuated with steady supersonic underexpanded jet and be used for high-speed flow mixing, and control applications.

# Acknowledgments

National Science Foundation supports this work through grant 1900177. The authors thank Dr. Phillip Kreth, University of Tennessee Space Institute, TN, for supporting this study.

#### References

- 1. B. Ritchie, D. Mujumdar, and J. Seitzman, "Mixing in co-axial jets using synthetic jet actuators," AIAA-2000-04-04.
- 2. Davis, S. A. & Glezer, A., "Mixing Control of Fuel Jets Using Synthetic Jet Technology: Velocity Field Measurements," AIAA Paper 99-0447.
- 3. Broadwell, J. E. and Mungal, M. G., "Large Scale Structures and Molecular Mixing," Physics Fluids, 1193-1206, 1991.
- 4. Kraus, D. K., and Cutler, A. D., "Mixing of Swirling Jets in a Supersonic Duct Flow," Journal of Propulsion and Power, Vol. 12, No. 1, 1995, pp. 170–177. doi:10.2514/3.24007
- 5. Cutler, A. D., and Doerner, S. E., "Effects of Swirl and Skew upon Supersonic Wall Jet in Crossflow," Journal of Propulsion and Power, Vol. 17, No. 6, 2001, pp. 1327–1332. doi:10.2514/2.5882
- 6. Drozda, T. G., Baurle, R. A., and Drummond, J. P., "Impact of Flight Enthalpy, Fuel Stimulant, and Chemical Reactions on the Mixing Characteristics of Several Injectors at Hypervelocity Flow Conditions," NASA Langley Research Center, May 2016, https://ntrs.nasa.gov/archive/nasa/casi.ntrs.nasa.gov/20160009131.pdf [retrieved May 2017].
- 7. Gruber, M. R., Nejad, A. S., Chen, T. H., and Dutton, J. C., "Transverse Injection from Circular and Elliptic Nozzles into a Supersonic Crossflow," Journal of Propulsion and Power, Vol. 16, No. 3, 2000, pp. 449–457. doi:10.2514/2.5609
- 8. VanLerberghe, W. M., Santiago, J. G., Dutton, J. C., and Lucht, R. P., "Mixing of a Sonic Transverse Jet Injected into a Supersonic Flow," AIAA Journal, Vol. 38, No. 3, 2000, pp. 470–479. doi:10.2514/2.984
- 9. Shigeru, A., ArifNur, H., Shingo, M., Kei, I., and Yasuhiro, T., "Fundamental Study of Supersonic Combustion in Pure Air Flow with Use of Shock Tunnel," Acta Astronautica, Vol. 57, Nos. 2–8, 2005, pp. 384–389. doi:10.1016/j.actaastro.2005.03.055
- 10. Menon, S., "Shock Wave Induced Mixing Enhancement in Scramjet Combustors," AIAA Paper 1989-0104, 1989. doi:10.2514/6.1989-104
- 11. Ben-Yakar, B., Mungal, M. G., and Hanson, R. K., "Time Evolution and Mixing Characteristics of Hydrogen and Ethylene Supersonic Crossflow," Physics of Fluids, Vol. 18, No. 2, 2006, Paper 026101. doi:10.1063/1.2139684
- 12. Hsu, K., Carter, C. D., Gruber, M. R., and Tam, C., "Mixing Study of Strut Injectors in Supersonic Flows," AIAA Joint Propulsion Conference, AIAA Paper 2009-5226, 2009. doi:10.2514/6.2009-5226
- 13. Hongbin, G., Zhi, L., Fei, L., Lihong, C., Shenglong, G., and Xinyu, C., "Characteristics of Supersonic Combustion with Hartmann-Sprenger Tube Aided Fuel Injection," AIAA Conference, AIAA Paper 2011-2326, 2011. doi:10.2514/6.2011-2326
- 14. Solomon, J. T., Cairnes, K., Nayak, C., Jones, M. and Alexander, D. Design and Characterization of Nozzle Injection Assemblies Integrated High-frequency Microactuators. AIAA Journal Vol. 56, No. 9, pp. 3436-3448, 2018.
- 15. Ali MY, Arora N, Topolski M, Alvi FS, and Solomon JT. Properties of Resonance Enhanced Microjets in Supersonic Crossflow" AIAA Journal, AIAA Journal, Vol. 55, No. 3, pp. 1075-1081. https://doi.org/10.2514/1.J055082, 2017.
- 16. Uzun, A., Solomon, J.T., Foster, C.H., Oates, W.S., Hussaini, M.Y., Alvi, F.S. Flow physics of a pulsed microjet actuator for high-speed flow control. AIAA Journal Volume 51, No. 12, pp 2894-2918, 2013.
- 17. Solomon, J. T., Foster, C., and Alvi F.S. Design, and characterization of High-Bandwidth, Resonance Enhanced, Pulsed Microactuators: A parametric study. AIAA Journal, Volume 51, No. 2, pp 386-396., 2013.
- 18. Solomon, J. T., Kumar, R., and Alvi, F.S. "High-Bandwidth Pulsed Microactuators for High-Speed Flow Control," AIAA Journal, Vol. 48, No. 10, pp. 2386-2396, doi.org/10.2514/1.J050405, 2010.
- 19. Solomon, J, T. High-bandwidth Unsteady Actuators for Active Control of High-Speed Flows," Ph.D. Dissertation, Florida State University. http://purl.flvc.org/fsu/fd/FSU\_migr\_etd-1642, 2010.
- 20. J.E. Jenkins, P.A. Kreth, J.T. Solomon, "Experimental investigation of a high-frequency pulsed co-axial injector using optical diagnostics" AIAA-4240 Aviation Meeting-, San Diego 2023.
- 21. J.T. Solomon, N. Hackworth, R. Lockyer, U. Philip, P. Kreth, "Velocity and vorticity fields of a High-Frequency pulsed supersonic co-axial injector" AIAA-4239 Aviation Meeting, San Diego 2023
- 22. J. T. Solomon, R. Lockyer, T. Jones, P. Kreth, "High-Frequency Pulsed Co-axial Injectors for High-Speed Flow Mixing and Control," AIAA Journal, Vol. 61, No. 12, pp 5332-5345, 2023
- 23. Lozano, A., Smith, S. H., Mungal, M. G. and Hanson, R. K., "Concentration Measurements in a Transverse Jet by Planar Laser-Induced Fluorescence of Acetone" AIAA Journal 32, 218-221, 1994.
- 24. Lozano, A., Yip, B., and Hanson, R. K., "Acetone: a by planar laser-induced fluorescence," Experiments in Fluids 13, 369-376, 1992